

# Transient Salt-Bridge-Based Supramolecular Polymers: Experiments and Theory

Gabriele Melchiorre, Matteo Valentini, Francesco Ranieri, Davide Cantiello, Roberta Cacciapaglia, Laura Baldini, Gianfranco Ercolani,\* and Stefano Di Stefano\*



Cite This: *J. Am. Chem. Soc.* 2026, 148, 6638–6645



Read Online

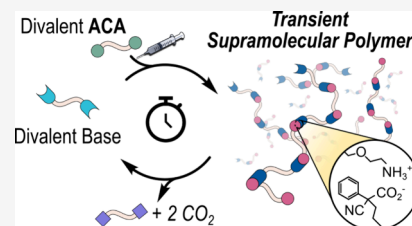
ACCESS |

Metrics & More

Article Recommendations

Supporting Information

**ABSTRACT:** The smooth decarboxylation under basic conditions of activated carboxylic acids (ACAs) is exploited to achieve a transient supramolecular polymer based on hydrogen bonds reinforced by electrostatic interactions. In particular, it is proved that when the aliphatic  $\alpha,\omega$ -diamine **3**, namely, 1,8-diamino-3,6-dioxaoctane, reacts with an equimolar amount of the activated dicarboxylic acid **1H<sub>2</sub>**, *i.e.*, a difunctional derivative of 2-cyano-2-phenylpropanoic acid, a supramolecular polymer of the kind –AB–BA–AB– is immediately formed in chloroform solution. The A–A and B–B monomers are held together by salt bridges (hydrogen bonds reinforced by electrostatic interactions) between ammonium and carboxylate functions. The larger the concentration of the added materials, the higher the polymerization degree (DP) of the polymer. Under the given experimental protocol, such a polymer disaggregates over time due to decarboxylation, and at the end of the process, only diamine **3** and waste product **4**, which cannot interact with one another anymore, remain in the solutions. DOSY spectra recorded at different reaction times definitely demonstrate the phenomenology described above. The trend of the degree of polymerization as a function of monomer concentration has been clarified in the light of the ring–chain equilibrium theory. The application of the theory enables the accurate evaluation of the distribution of linear and cyclic oligomers as well as the critical concentration,  $c_{crit}$ , above which polymerization rapidly becomes more extensive due to the saturation of macrocyclic species. Notably, the ACA is not used just as a stimulus for a dissipative system, but as one of its structural components.



## INTRODUCTION

Chemically time-programmable systems are receiving increasing interest from the scientific community due to several reasons, including the possible achievements of (i) smart materials able to respond to external stimuli (soft robotics and self-healing polymers),<sup>1</sup> (ii) artificial life-like systems able to evolve in response to changes of the environmental conditions,<sup>2</sup> and (iii) molecular machines (switches and motors) capable of performing particular tasks and the like.<sup>3</sup> Time programming often requires the dissipation of a chemical species, which is generally defined as a stimulus. Activated carboxylic acids (ACAs)<sup>4</sup> have been recently used to program over time the operation of many chemical systems based on the acid–base reaction, ranging from host–guest pairs,<sup>5</sup> catalysts,<sup>6</sup> smart materials,<sup>1f,7</sup> dynamic libraries,<sup>8</sup> molecular machines,<sup>3a,3c,9</sup> and supramolecular polymers.<sup>10</sup> Such systems generally operate under dissipative conditions, with no energy transferred from the stimulus to the system;<sup>11</sup> however, sometimes, this transfer occurs and an energy ratchet operates.<sup>7c,9b,10,12</sup> This is the case of recently reported transient supramolecular polymers<sup>13</sup> based on imine chemistry, where tribromoacetic acid (the ACA stimulus) drives a transamination reaction,<sup>10</sup> which, in turn, gives rise to the formation of polymers whose monomers are held together through hydrogen bonding interactions between ammonium cations

and crown-ether moieties. When the stimulus is consumed, the ammonium cations are converted to free, neutral amine functions and the polymer falls apart. However, in this case, warming of the solution is necessary to revert to the initial conditions since, in the absence of tribromoacetic acid (that is, when the stimulus is exhausted), a strong deceleration of the back-transamination necessary to restore the initial composition is observed. Tribromoacetic acid is in fact a catalyst for the back-transamination, and when it is exhausted, the system ends up in a kinetic trap.

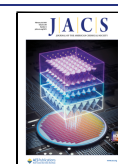
Here, we report a new strategy for achieving a transient supramolecular polymer from two symmetrical monomers, A–A and B–B, where no stimulus is required to form or decompose the polymer. After addition, the two monomers react with each other through an acid–base reaction that activates both the immediate formation of the polymer and its slower depolymerization.

**Received:** December 10, 2025

**Revised:** January 23, 2026

**Accepted:** January 27, 2026

**Published:** February 4, 2026



## GENERAL DESIGN

Figure 1A shows the operation principle of a generic dissipative system driven by an ACA ( $\text{RCO}_2\text{H}$ ). Initially, a Brønsted base

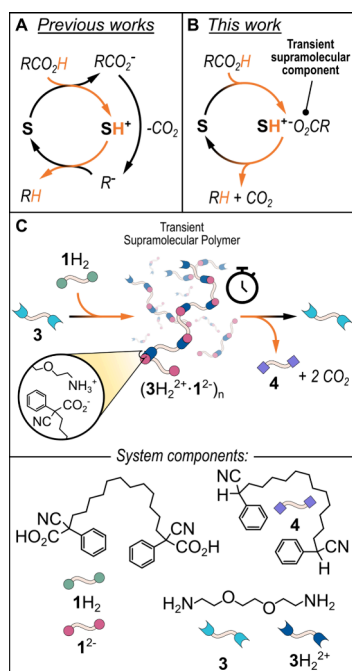


**Figure 1.** (A) Schematic representation of an acid–base-operated system driven by the decarboxylation of an ACA. (B) General operation scheme exploited in this work, in which the ACA is used as a structural component of the transient dissipative system. (C) Schematic cartoon and relative molecular structures that depict the transient formation of a salt-bridge-based supramolecular polymer generated from a difunctional ACA ( $1\text{H}_2$ ) and a diamine ( $3$ ).

site in the system ( $S$ ) receives a proton from the ACA and passes to the protonated state  $\text{SH}^+$ . The conjugated base of the ACA, ( $\text{RCO}_2^-$ ), is not stable and loses  $\text{CO}_2$  to be transformed into a carbanion ( $\text{R}^-$ ), which is a strong base that takes back the proton from  $\text{SH}^+$  to restore  $S$  in the initial neutral form. In other words, the ACA is a tool to modulate over time the acidity of the environment and hence the protonation state of the basic site present in  $S$ .

In the present case, the role of the ACA is different, as illustrated in Figure 1B. Here, after proton donation, its conjugate base ( $\text{RCO}_2^-$ ) will be a structural component of the dissipative system, which will be transient in nature, given the tendency of the carboxylate anion to lose  $\text{CO}_2$ . Thus, the ACA not only determines the temporary existence of a non-equilibrium state but also enters in the chemical structure of such non-equilibrium state as a molecular unit.<sup>14</sup> More in detail, we use the difunctional ACA  $1\text{H}_2$  to transiently generate a salt-bridge-based supramolecular polymer, as shown in Figure 1C. Under basic conditions and using an aprotic solvent,  $1\text{H}_2$  should decarboxylate smoothly, exactly like its monofunctional parent 2-cyano-2-phenylpropanoic acid  $2\text{H}$ . The idea is to add equimolar amounts of ACA  $1\text{H}_2$  and diamine  $3$  in a chloroform solution to cause a proton transfer from the acidic carboxylic functions of  $1\text{H}_2$  to the basic amine functions of  $3$ . Such functions are now activated in the form of carboxylate anions and ammonium cations, respectively, for giving rise to a supramolecular polymer whose monomers are held together by salt bridge interactions,<sup>15</sup> where hydrogen bonding is reinforced by electrostatic attraction. However, the carboxylate anions should be unstable under the adopted conditions, and due to decarboxylation and consequent back-proton transfer, the polymer should disappear over time leaving in solution neutral  $3$  and  $4$ , incapable of interacting with each other.

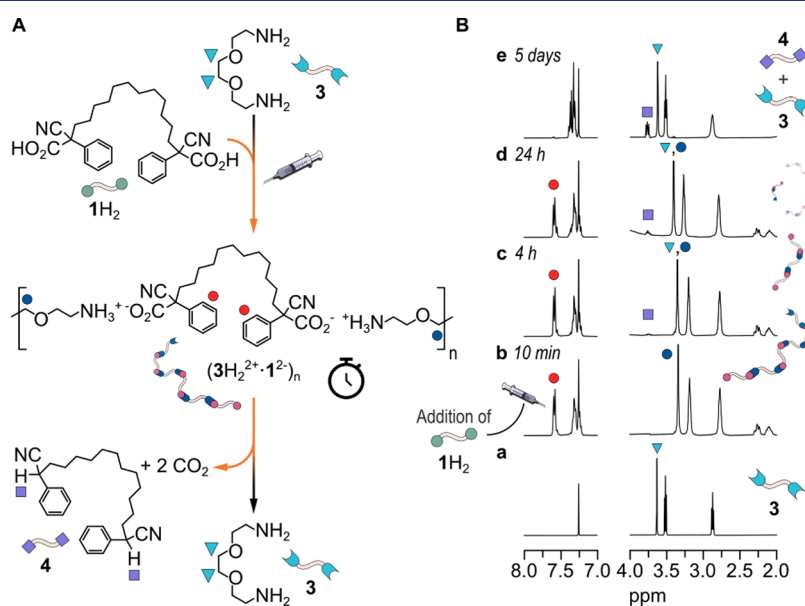


**Figure 2.** (A) Schematic representation of the diamine  $3$  that, after being protonated by the difunctional ACA ( $1\text{H}_2$ ), gives rise to a supramolecular polymer in which the bis-deprotonated ACA ( $1^{2-}$ ) is a structural component. The decarboxylation reaction that occurs over time breaks apart the assembly, releasing the starting diamine  $3$  and the decarboxylated product  $4$ , which are unable to interact with each other. (B)  $^1\text{H}$  NMR monitoring of a solution containing the diamine  $3$  ( $10\text{ mM}$ ) depicted in (A) before (trace *a*,  $t = 0$ ) and after (from trace *b* to trace *e*) the addition of  $10\text{ mM}$  ACA  $1\text{H}_2$  ( $\text{CDCl}_3$ ,  $25\text{ }^\circ\text{C}$ ; see (A) for the color code), demonstrating the ability of  $3$  to catalyze the decarboxylation of the ACA over the time.

## RESULTS AND DISCUSSION

### Experiments

ACA 1H<sub>2</sub> was prepared in two steps. First, commercially available ethyl 2-cyano-2-phenylacetate and 1,12-dibromodecane were reacted in DMSO (50 °C for 6 h) in the presence of K<sub>2</sub>CO<sub>3</sub> and catalytic KI. Then, the resulting diester, purified through column chromatography (see the Supporting Information (SI) for details), was hydrolyzed in EtOH/H<sub>2</sub>O 15:4 (RT, for 1 day) in the presence of KOH (strong hydrogen bonding of the resulting carboxylate with the solvent protects the former from decarboxylation). Acidification with sulfuric acid causes the precipitation of 1H<sub>2</sub>, which was purified and fully characterized.

A series of experiments were initially carried out in the low concentration domain to find the optimal conditions for a conveniently fast decarboxylation of 1H<sub>2</sub>. The choice of the noncompetitive chloroform as a solvent was dictated by the need to favor salt-bridge interactions, on which, in our design, the supramolecular polymer is based. However, since a strong salt-bridge interaction may also retard the decarboxylation of 1, which can become unsustainably slow, a compromise must be found.

First, 10 mM 1H<sub>2</sub> was added to 20 mM monofunctional butylamine 5 in CDCl<sub>3</sub> in an NMR tube at room temperature (see Figure S18). Immediately after addition, shifts of diagnostic signals of both 1H<sub>2</sub> and 5 revealed proton transfer from the carboxylic functions of 1H<sub>2</sub> to the amino function of 5. However, no sign of decarboxylation was detected in the following 8 h. We ascribed this result to the strong ion pairing of (SH<sup>+</sup>)<sub>2</sub>•I<sup>2-</sup>, which retards the decarboxylation, stabilizing the carboxylate function. In fact, decarboxylation was observed to occur and finish in 2 days when carried out in the more competitive CDCl<sub>3</sub>/CD<sub>3</sub>CN 83:17 solvent mixture, where the ion pairing is weakened (see Figure S19).

To our pleasure, we discovered that when 10 mM 1H<sub>2</sub> was reacted with 10 mM diamine 3,<sup>16</sup> the decarboxylation proceeded even in pure CDCl<sub>3</sub>, although 5 days were needed for the complete disappearance of 1H<sub>2</sub> to give the decarboxylated product 4 (see Figure 2A,B). The higher reactivity of 1H<sub>2</sub> toward decarboxylation when 3 is used instead of 5 is very likely due to the presence of the oxygen atoms in 3, which compete with the carboxylate functions for the hydrogen bonding with the ammonium heads.<sup>17</sup>

Trace *a* of Figure 2B is related to 10 mM 3, while trace *b*, which is recorded 10 min after the addition of 1H<sub>2</sub>, clearly shows that the acid–base reaction between 1H<sub>2</sub> and 3 has occurred (refer to Figure 2A for signal assignment). From now onward, decarboxylation occurs (traces *b* to *e*) and, after 5 days (trace *e*), the reaction is complete with the signals of 3 restored at the initial chemical shift values.

Next, a series of experiments at higher and equimolar concentrations of 1H<sub>2</sub> and 3 were performed to achieve a transient supramolecular polymer. The experimental protocol consisted of adding equimolar amounts of 1H<sub>2</sub> and 3 in CDCl<sub>3</sub> in a series of NMR tubes at increasing concentration. Since the decarboxylation is slow enough (it lasts 5 days; see above), the bidimensional DOSY spectra of the different tubes taken immediately after the addition of 1H<sub>2</sub> and 3 give a measure of the initial weight-average polymerization degree (DP) of the (3H<sub>2</sub><sup>2+</sup>•I<sup>2-</sup>)<sub>*n*</sub> polymers present in each tube.

Table 1 reports the DPs obtained from diffusion coefficients (*D*<sub>obs</sub>) recorded at different and equimolar concentrations following eq 1.

$$DP = \left( \frac{D_{\text{monomer}}}{D_{\text{obs}}} \right)^2 \quad (1)$$

**Table 1. Initial Diffusion Coefficients (*D*<sub>obs</sub>) for 1:1 Mixtures of 1H<sub>2</sub> and 3 at Different Concentrations (*c*<sub>0</sub>), and Weight-Average Degree of Polymerizations (DP) Calculated by eq 1**

<i>c</i> <sub>0</sub> (mM)	<i>D</i> <sub>obs</sub> (cm <sup>2</sup> /s) <sup>a</sup>	DP <sup>b</sup>
5	5.77 × 10 <sup>-6</sup>	4.3
10	5.78 × 10 <sup>-6</sup>	4.2
30	5.67 × 10 <sup>-6</sup>	4.4
50	2.34 × 10 <sup>-6</sup>	26
60	2.28 × 10 <sup>-6</sup>	27
80	1.69 × 10 <sup>-6</sup>	50
100	1.20 × 10 <sup>-6</sup>	98
150	7.28 × 10 <sup>-7</sup>	267
200	5.66 × 10 <sup>-7</sup>	442

<sup>a</sup>Relative error is below ±2%. <sup>b</sup>Calculated relative error is ±6%.

This last equation was derived following a recent approach,<sup>18</sup> where the squared power is just an empirical value that has been shown to fit well the behavior of polymers in CDCl<sub>3</sub> (see the SI for the derivation of eq 1). The squared power has also been associated with a rod-like shape of the molecules in solution, as opposed to a spherical shape that would require the cubic power.<sup>19</sup> We remark, however, that the exponent in eq 1 is purely empirical, and we do not suggest any specific shape of the polymer. It is worth noting that a cubic exponent would give unreasonably high DP values.<sup>20</sup> The reference *D*<sub>monomer</sub> was chosen as the average of the diffusion coefficients related to 5.0 mM solutions of 1H<sub>2</sub> (*D*<sub>obs</sub> = 8.10 × 10<sup>-6</sup> cm<sup>2</sup>/s) and 3 (*D*<sub>obs</sub> = 1.56 × 10<sup>-5</sup> cm<sup>2</sup>/s), i.e., *D*<sub>monomer</sub> = 1.19 × 10<sup>-5</sup> cm<sup>2</sup>/s. A 5.0 mM solution of 4 gave a *D*<sub>obs</sub> value of 8.91 × 10<sup>-6</sup> cm<sup>2</sup>/s, very similar to that of 1H<sub>2</sub>, strongly pointing to the absence of any aggregation when 1H<sub>2</sub> is the only species present in solution at a concentration as low as 5.0 mM.

After recording the DOSY spectra, the solutions were kept at room temperature for 24 h and then warmed to 50 °C to prevent the formation of a precipitate, which otherwise would be observed after 48 h, in the more concentrated samples (*c*<sub>0</sub> ≥ 80 mM).<sup>21</sup> The appearance of the precipitate precluded the reversibility of the system. In contrast, following the above procedure (24 h at room temperature and then heating to 50 °C), no phase separation is ever observed in any samples, and the decarboxylation is complete after a total of 48 h (thus 24 h at RT, plus 24 h at 50 °C) with high reproducibility. For example, Figure 3 reports the NMR monitoring of the reaction between 100 mM 1H<sub>2</sub> and 100 mM 3, when the above protocol is followed (see the SI, Figures S20–S28 for the experiments at different concentrations).

It is evident that at the end of the decarboxylation (after a total of 48 h), diamine 3 is recovered in its neutral form while 1H<sub>2</sub> is completely converted into product 4. Since 3 and 4 cannot interact with each other, the supramolecular polymer disappears from the solution. Interestingly, the degree of polymerization drops to low values, long before the

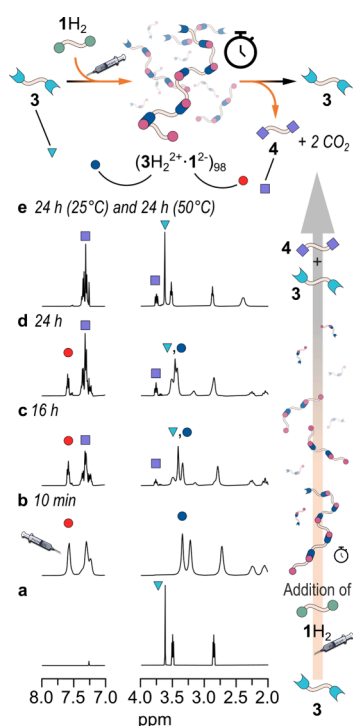


**Figure 3.** Schematic cartoon showing the transient formation of a supramolecular polymer obtained by mixing equimolar amounts of the symmetric divalent ACA  $1\text{H}_2$  and the diamine **3**. Its formation can be monitored via  $^1\text{H}$  NMR. Indeed, after the addition to a solution containing 100 mM diamine **3** (trace *a*,  $t = 0$ , blue triangle) of the ACA  $1\text{H}_2$  (from trace *b* to trace *e*), a shift in the diamine signals is observed, suggesting the formation of the supramolecular polymer  $((3\text{H}_2^{2+} \bullet 1^{2-})_n$ , red and blue circles, corresponding to the difunctional ACA conjugated base and protonated diamine, respectively), which is also confirmed by DOSY experiments. Its subsequent breakdown can also be monitored by observing the appearance of the decarboxylated product **4** (violet square) over time ( $\text{CDCl}_3$ ,  $25^\circ\text{C}$  for 24 h and then additional 24 h at  $50^\circ\text{C}$ , whole spectra in Figures S29 and S30; see the cartoon for the color code).

decarboxylation reaction is complete (vide infra). This behavior is due, not only to the decreasing concentration of active bifunctional monomers, but mainly to the intermediate formation of monofunctional monomers (semidecarboxylated and semiprotonated chains) that act as stoppers, inhibiting chain growth.

Before giving even more convincing evidence of what is occurring in the solutions, let us sum up results and explanations exposed so far: (i) a supramolecular polymer is formed when  $1\text{H}_2$  and **3** are added in equimolar amounts to the solution due to proton transfer and establishing of salt bridges; (ii) the larger the amount of equimolar  $1\text{H}_2 + 3$  added, the higher the DP of the polymer; (iii) after 24 h at room temperature and additional 24 h at  $50^\circ\text{C}$ , the decarboxylation process is over and the supramolecular polymer disappears.

DOSY experiments resolved over time provide final and clear-cut evidence of our interpretation of the observed phenomenology. Figure 4a–c reports, in the typical logarithmic scale, the bidimensional DOSY spectra recorded at (a) 20 min, (b) 24 h, and (c) 48 h (with the sample held at  $50^\circ\text{C}$  for the last 24 h) after mixing 200 mM  $1\text{H}_2$  and 200 mM **3** in  $\text{CDCl}_3$ . The lowest value of  $D_{\text{obs}}$  is observed immediately after the addition of the materials ( $5.66 \times 10^{-7}$

$\text{cm}^2/\text{s}$ , which corresponds to  $\text{DP} = 442$ ), and then, after 24 h at room temperature, it increases to  $2.20 \times 10^{-6} \text{ cm}^2/\text{s}$  ( $\text{DP} = 29$ ) and still increases to  $6.72 \times 10^{-6} \text{ cm}^2/\text{s}$  ( $\text{DP} = 3$ ) after an additional 24 h at  $50^\circ\text{C}$ . In other words, the supramolecular polymer  $(3\text{H}_2^{2+} \bullet 1^{2-})_n$  with  $\text{DP} = 442$ , immediately formed after addition of the monomers, has completely vanished after 24 h at  $25^\circ\text{C}$  and additional 24 h at  $50^\circ\text{C}$ . Figure 4d and Figure 4e show the corresponding signals on a linear scale for the DOSY spectra at  $t = 20$  min and  $t = 48$  h, respectively (Figure 4a and Figure 4c show the same spectra on a logarithmic scale, respectively). While in the first case, a unique, slightly disperse distribution of heavy species involving both monomers is apparent, in the second case, two light noninteracting species are clearly distinguishable, corresponding to products **3** and **4**.

### Theory

The data in Table 1 show that DP increases very slowly at low monomer concentrations up to a critical concentration, around 70–80 mM, after which it increases very sharply. This behavior can be understood in the light of the theory of ring–chain equilibria presented by Jacobson and Stockmayer (JS) as early as 1950<sup>22</sup> and successively restated to make it more understandable outside the community of polymer chemists.<sup>23</sup> An even more straightforward version of the theory applied to the specific case of equimolar A–A and B–B polymerizations is reported in the SI. According to the theory, two monomers of the types A–A and B–B, capable of reacting reversibly with each other, give rise to an equilibrium mixture of linear and cyclic oligomers whose distribution depends on the monomer concentration  $c_0$ , the intermolecular equilibrium constant for the reaction between the end groups  $K$ , and the effective molarities  $\text{EM}_i$  of the rings being formed. The latter parameter is defined as the ratio  $K_{(\text{intra})i}/K$ , where  $K_{(\text{intra})i}$  is the intramolecular equilibrium constant for the ring-closing reaction leading to the cyclic  $i$ -mer. It measures the cyclization tendency of the linear precursor of the ring independently of the reactivity of its end groups.<sup>24</sup> JS have shown that for a series of strainless cyclic oligomers formed from long chains obeying Gaussian statistics (say longer than 25–30 skeletal bonds), the equilibrium effective molarity,  $\text{EM}_i$ , varies inversely with the  $5/2$  power of the oligomerization degree as shown by eq 2, where the factor  $B$  corresponds to the effective molarity of the smallest cyclic oligomer.<sup>22,23</sup>

$$\text{EM}_i = B i^{-5/2} \quad (2)$$

In the present case, all of the cyclic oligomers  $c-(1^{2-} \bullet 3\text{H}_2^{2+})_i$  are large enough to follow eq 2. Accordingly, the mass balance equation in terms of the monomeric units of one kind is given by eq 3, where  $x$  is the extent of reaction in the chain fraction.

$$c_0 = B \sum_{i=1}^{\infty} i^{-3/2} x^{2i} + \frac{x}{2K(1-x)^2} \quad (3)$$

The two terms in the right-hand side of eq 3 represent the amount of monomer of one kind in the ring ( $c_r$ ) and chain ( $c_c$ ) fractions, respectively. When the intermolecular constant  $K$  is very large, eq 3 predicts the phenomenon of the critical concentration,  $c_{\text{crit}}$ . It is the monomer concentration below which all the monomers go into the cyclic fraction, and above which the cyclic fraction stops growing and all the monomers go into the chain fraction.<sup>22,23</sup> This phenomenon occurs because a very large  $K$  value assures that  $c_c$  is always negligible

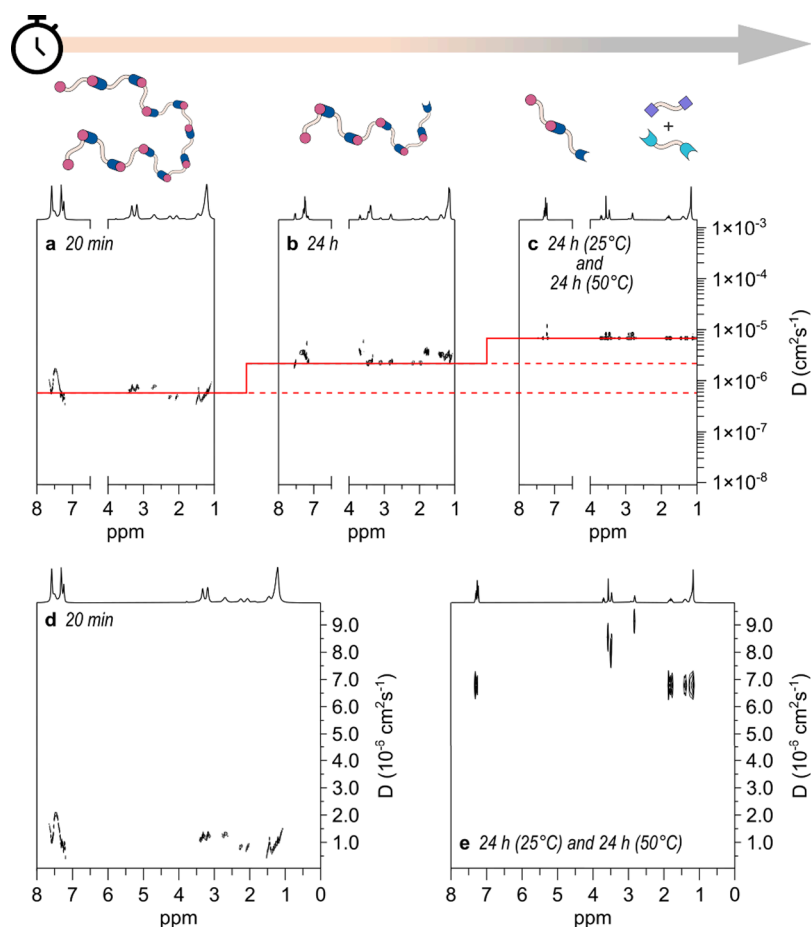


**Figure 4.** Time-resolved DOSY experiments. DOSY of a solution of 200 mM  $1H_2$  and 200 mM **3** in  $CDCl_3$  was taken at (a) 20 min, (b) 24 h, and (c) 48 h (with the sample held at 50 °C for the last 24 h) after mixing of the reagents on a typical logarithmic scale. Spectra (d) and (e) correspond to selected regions of spectra (a) and (c), respectively, put on a linear scale.

until  $x$  is very close to 1, whereas  $c_r$  converges to  $c_{crit} = 2.612B$  for  $x$  tending to 1,<sup>25</sup> meaning that the cyclic fraction, in contrast with the chain fraction, can only contain a limited number of monomeric units.

JS have shown that for equimolar concentrations of A—A and B—B (the case they call the “equivalent” polymer), the weight-average degree of polymerization is given by eq 4, where  $DP_r$  and  $DP_c$ , given by eqs 5 and 6, are the weight-average degrees of polymerization of the ring and chain fractions, respectively (see also the SI for the derivation of eqs 4–6).

$$DP = \frac{c_r DP_r + c_c DP_c}{c_0} \quad (4)$$

$$DP_r = \frac{2 \sum_{i=1}^{\infty} i^{-1/2} x^{2i}}{\sum_{i=1}^{\infty} i^{-3/2} x^{2i}} \quad (5)$$

$$DP_c = \frac{1+x}{1-x} \quad (6)$$

Considering eqs 3 and 4, the data of DP vs  $c_0$  from Table 1 have been fitted by a least-squares procedure to optimize the values of  $B$  and  $K$  [optimized values are  $B = (3.1 \pm 0.1) \times 10^{-2} \text{ mol L}^{-1}$  and  $K = (4.4 \pm 0.1) \times 10^5 \text{ mol}^{-1} \text{ L}$ ; see the SI for details]. The fit of the calculated curve to the experimental data, shown in Figure 5, is remarkably good, supporting eq 4

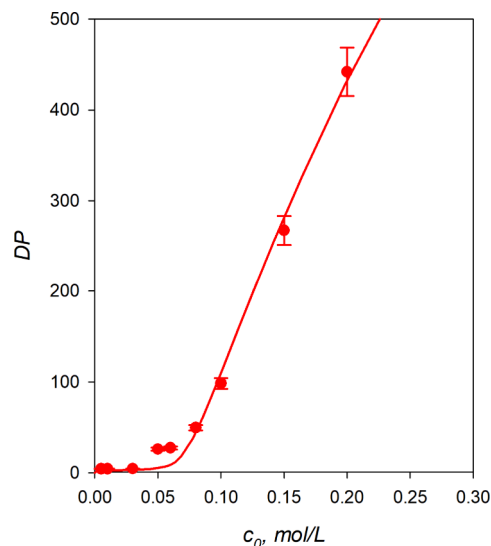


**Figure 5.** Plot of the initial weight-average degree of polymerization, DP, against the monomer concentration,  $c_0$ . The points are experimental, and the curve is calculated using eqs 3 and 4 with the optimized values of  $B$  and  $K$ .

and the presence of ring–chain equilibria in solution. The calculated critical concentration,  $c_{crit} = 8.1 \times 10^{-2} \text{ mol L}^{-1}$ ,

corresponds to the  $c_0$  value where the chain fraction steeply grows.

It is worth noting that in the case of ring–chain equilibria, the number-average degree of polymerization, in contrast to the weight-average degree of polymerization, is always very low. Indeed, at high  $c_0$  values, the ring fraction is scarcely significant on a weight basis but makes a substantial contribution to the total number of molecules and, hence, markedly lowers the overall number-average degree of polymerization. This will be particularly true when  $x$  is close to 1 and the number of chain polymer molecules is consequently small.

One might wonder how significant the values of  $B$  and  $K$  obtained from the fit are. Regarding the value of  $B$ , it is interesting to compare the obtained value with that estimated by a practical method suggested by Mandolini for large rings (see the SI for details).<sup>24c,24d,24f</sup> The method is based on eq 7, where  $\nu$  is the number of rotatable single bonds present in the smallest cyclooligomers and  $\sigma$  is its symmetry number accounting for the number of equivalent bonds available for ring opening.

$$B = \frac{6.63}{\sigma} \nu^{-3/2} \quad (7)$$

In the present case,  $\nu = 24$  and  $\sigma = 2$ ; thus, a value of  $B = 2.8 \times 10^{-2} \text{ mol L}^{-1}$  can be calculated, which is in very good agreement with that obtained by fitting the experimental DP values. As to the value of  $K$ , we tried to measure its value directly by titrating butylamine **5** with **2H** in deuterated chloroform at room temperature. The association constant between  $5\text{H}^+$  and  $2^-$  is so strong that only a lower limit for  $K$  ( $\geq 10^5 \text{ mol}^{-1} \text{ L}$ ) could be estimated (see Figure S34). The same result was found when diamine **3** was rapidly (to avoid decarboxylation) titrated with monofunctional acid **2H**. Again, the binding (1:2) between  $3\text{H}_2^{2+}$  and  $2^-$  was too strong to measure (see Figure S36 and related details). However, this limit is in full accordance with the value of  $K$  obtained by the fitting procedure.

## CONCLUSIONS

In this report, we show that a transient, salt-bridge based supramolecular polymer can be obtained by the simple reaction of equimolar amounts of a diamine and a divalent activated dicarboxylic acid. Upon addition of the reagents, the supramolecular polymer is initially formed and then slowly decomposes due to decarboxylation under the given experimental conditions. Time-resolved DOSY spectroscopy allows the polymer's disaggregation to be followed over time. The experimental data recorded immediately after the addition of the reagents allowed for the determination of the initial polymerization degree as a function of the monomer concentration. The obtained curve is fitted remarkably well by a model of reversible polymerization that accounts for the formation of cyclic oligomers. To the best of our knowledge, such a fitting has no precedent in the literature. The model, initially proposed by Jacobson and Stockmayer,<sup>22</sup> and subsequently revisited to highlight the role played by the equilibrium constant  $K$  for linear propagation,<sup>23</sup> is presented here for the specific case of equimolar A–A and B–B polymerizations, in a version that should be easily understandable even by nonexperts.

It is remarkable that an activated dicarboxylic acid has been used here, not only as a stimulus to control a dissipative

polymer over time but also as a building block of the polymer itself. Finally, given the importance of salt-bridge interactions in biochemistry, particularly in the stabilization of protein structures,<sup>26</sup> the possible use of ACAs to temporarily control their conformations should not be overlooked.

## ASSOCIATED CONTENT

### Supporting Information

The Supporting Information is available free of charge at <https://pubs.acs.org/doi/10.1021/jacs.5c22087>.

Instruments, materials and methods, synthesis, NMR, UV–Vis, and FTIR-ATR spectra of newly synthesized compounds, NMR kinetic spectra, DOSY spectra, NMR titrations, theory of ring–chain equilibria, estimation of  $B$  and  $K$  values, and derivation of eq 1 (PDF)

## AUTHOR INFORMATION

### Corresponding Authors

**Gianfranco Ercolani** – Dipartimento di Scienze e Tecnologie Chimiche, Università di Roma Tor Vergata, Roma 00133, Italy; [orcid.org/0000-0003-2437-3429](https://orcid.org/0000-0003-2437-3429); Email: [ercolani@uniroma2.it](mailto:ercolani@uniroma2.it)

**Stefano Di Stefano** – Dipartimento di Chimica and Istituto per i Sistemi Biologici - CNR (ISB-CNR), Sede Secondaria di Roma - Meccanismi di Reazione, c/o Dipartimento di Chimica Università di Roma La Sapienza, Rome I-00185, Italy; [orcid.org/0000-0002-6742-0988](https://orcid.org/0000-0002-6742-0988); Email: [stefano.distefano@uniroma1.it](mailto:stefano.distefano@uniroma1.it)

### Authors

**Gabriele Melchiorre** – Dipartimento di Chimica and Istituto per i Sistemi Biologici - CNR (ISB-CNR), Sede Secondaria di Roma - Meccanismi di Reazione, c/o Dipartimento di Chimica Università di Roma La Sapienza, Rome I-00185, Italy

**Matteo Valentini** – Dipartimento di Chimica and Istituto per i Sistemi Biologici - CNR (ISB-CNR), Sede Secondaria di Roma - Meccanismi di Reazione, c/o Dipartimento di Chimica Università di Roma La Sapienza, Rome I-00185, Italy

**Francesco Ranieri** – Dipartimento di Chimica and Istituto per i Sistemi Biologici - CNR (ISB-CNR), Sede Secondaria di Roma - Meccanismi di Reazione, c/o Dipartimento di Chimica Università di Roma La Sapienza, Rome I-00185, Italy

**Davide Cantiello** – Dipartimento di Chimica and Istituto per i Sistemi Biologici - CNR (ISB-CNR), Sede Secondaria di Roma - Meccanismi di Reazione, c/o Dipartimento di Chimica Università di Roma La Sapienza, Rome I-00185, Italy

**Roberta Cacciapaglia** – Dipartimento di Chimica and Istituto per i Sistemi Biologici - CNR (ISB-CNR), Sede Secondaria di Roma - Meccanismi di Reazione, c/o Dipartimento di Chimica Università di Roma La Sapienza, Rome I-00185, Italy; [orcid.org/0000-0002-3119-4851](https://orcid.org/0000-0002-3119-4851)

**Laura Baldini** – Dipartimento di Scienze Chimiche, della Vita e della Sostenibilità Ambientale, Università degli Studi di Parma, Parma 43124, Italy; [orcid.org/0000-0002-0985-4331](https://orcid.org/0000-0002-0985-4331)

Complete contact information is available at: <https://pubs.acs.org/10.1021/jacs.5c22087>

## Author Contributions

The manuscript was written through the contributions of all authors.

## Funding

Funds used to support the research of the manuscript are from (i) Ateneo 2022 Sapienza (RG1221815C85AF91), (ii) PRIN project “Chemically-Driven Autonomous Molecular Machines and Other Dissipative Systems” (N° 2022X779 KE), and (iii) COMP-R Initiatives, the “Departments of Excellence” program of the Italian Ministry for Education, University and Research (MUR 2023–2027).

## Notes

The authors declare no competing financial interest.

## ABBREVIATIONS

ACA, activated carboxylic acid; <sup>1</sup>H NMR, proton nuclear magnetic resonance; DP, polymerization degree; 2D-DOSY, two-dimensional diffusion-ordered spectroscopy

## REFERENCES

- (1) (a) Boekhoven, J.; Hendriksen, W. E.; Koper, G. J. M.; Eelkema, R.; van Esch, J. H. Transient assembly of active materials fueled by a chemical reaction. *Science* **2015**, *349*, 1075–1079. (b) *Out-of-Equilibrium (Supra)molecular Systems and Materials*; Giuseppone, N.; Walther, A., Eds.; Wiley-VCH, 2021. (c) Kariyawasam, L. S.; Hossain, M. M.; Hartley, C. S. The Transient Covalent Bond in Abiotic Nonequilibrium Systems. *Angew. Chem., Int. Ed.* **2021**, *60*, 12648–12658. (d) Rodon-Fores, J.; Würbser, M. A.; Kretschmer, M.; Rieß, B.; Bergmann, A. M.; Lieleg, O.; Boekhoven, J. A chemically fueled supramolecular glue for self-healing gels. *Chem. Sci.* **2022**, *13*, 11411–11421. (e) Del Giudice, D.; Fratello, F.; Sappino, C.; Di Stefano, S. Chemical Tools for the Temporal Control of Water Solution pH and Applications in Dissipative Systems. *Eu. J. Org. Chem.* **2022**, *33*, No. e202200407. (f) Fusi, G.; Del Giudice, D.; Skarsetz, O.; Di Stefano, S.; Walther, A. Autonomous Soft Robots Empowered by Chemical Reaction Networks. *Adv. Mater.* **2023**, *35*, No. 2209870. (g) Pol, M. D.; Dai, K.; Thomann, R.; Moser, S.; Roy, S. K.; Pappas, C. G. Guiding Transient Peptide Assemblies with Structural Elements Embedded in Abiotic Phosphate Fuels. *Angew. Chem., Int. Ed.* **2024**, *63*, No. e202404360.
- (2) (a) Merindol, R.; Walther, A. Materials learning from life: concepts for active, adaptive and autonomous molecular systems. *Chem. Soc. Rev.* **2017**, *46*, 5588–5619. (b) Mishra, A.; Korlepara, D. B.; Kumar, M.; Jain, A.; Jonnalagadda, N.; Bejagam, K. K.; Balasubramanian, S.; George, S. J. Biomimetic temporal self-assembly via fuel-driven controlled supramolecular polymerization. *Nat. Commun.* **2018**, *9*, 1295. (c) Das, K.; Gabrielli, L.; Prins, L. J. Chemically Fueled Self-Assembly in Biology and Chemistry. *Angew. Chem., Int. Ed.* **2021**, *60*, 20120–20143. (d) Otto, S. An Approach to the De Novo Synthesis of Life. *Acc. Chem. Res.* **2022**, *55*, 145–155. (e) Cappelletti, D.; Lancia, F.; Basagni, A.; Đorđević, L. ATP-Regulated Formation of Transient Peptide Amphiphiles Superstructures. *Small* **2025**, *21*, No. 2410850.
- (3) (a) Borsley, S.; Leigh, D. A.; Roberts, B. M. W. Molecular Ratchets and Kinetic Asymmetry: Giving Chemistry Direction. *Angew. Chem., Int. Ed.* **2024**, *63*, No. e202400495. (b) Aprahamian, I.; Goldup, S. M. Non-equilibrium Steady States in Catalysis, Molecular Motors, and Supramolecular Materials: Why Networks and Language Matter. *J. Am. Chem. Soc.* **2023**, *145*, 14169–14183. (c) Biagini, C.; Di Stefano, S. Abiotic Chemical Fuels for the Operation of Molecular Machines. *Angew. Chem., Int. Ed.* **2020**, *59*, 8344–8354. (d) Wilson, M. R.; Solà, J.; Carlone, A.; Goldup, S. M.; Lebrasseur, N.; Leigh, D. A. An autonomous chemically fuelled small-molecule motor. *Nature* **2016**, *534*, 235–240. (e) Borodin, O.; Shchukin, Y.; Robertson, C. C.; Richter, S.; Von Delius, M. Self-Assembly of Stimuli-Responsive [2]Rotaxanes by Amidinium Exchange. *J. Am. Chem. Soc.* **2021**, *143*, 16448–16457.
- (4) (a) Del Giudice, D.; Di Stefano, S. Dissipative Systems Driven by the Decarboxylation of Activated Carboxylic Acids. *Acc. Chem. Res.* **2023**, *56*, 889–899. (b) Olivieri, E.; Quintard, A. Out of Equilibrium Chemical Systems Fueled by Trichloroacetic Acid. *ACS Org. Inorg. Au* **2023**, *3*, 4–12.
- (5) (a) Rispoli, F.; Spatola, E.; Del Giudice, D.; Cacciapaglia, R.; Casnati, A.; Baldini, L.; Di Stefano, S. Temporal Control of the Host–Guest Properties of a Calix[6]arene Receptor by the Use of a Chemical Fuel. *J. Org. Chem.* **2022**, *87*, 3623–3629. (b) Del Giudice, D.; Spatola, E.; Valentini, M.; Bombelli, C.; Ercolani, G.; Di Stefano, S. Time-programmable pH: decarboxylation of nitroacetic acid allows the time-controlled rising of pH to a definite value. *Chem. Sci.* **2021**, *12*, 7460–7466. (c) Ghosh, A.; Paul, I.; Schmittl, M. Multitasking with Chemical Fuel: Dissipative Formation of a Pseudorotaxane Rotor from Five Distinct Components. *J. Am. Chem. Soc.* **2021**, *143*, 5319–5323.
- (6) (a) Biagini, C.; Fielden, S. D. P.; Leigh, D. A.; Schaufelberger, F.; Di Stefano, S.; Thomas, D. Dissipative Catalysis with a Molecular Machine. *Angew. Chem., Int. Ed.* **2019**, *58*, 9876–9880. (b) Valiyev, I.; Ghosh, A.; Paul, I.; Schmittl, M. Concurrent base and silver(I) catalysis pulsed by fuel acid. *Chem. Commun.* **2022**, *58*, 1728–1731.
- (7) (a) Olivieri, E.; Gasch, B.; Quintard, G.; Naubron, J.-V.; Quintard, A. Dissipative Acid-Fueled Reprogrammable Supramolecular Materials. *ACS Appl. Mater. & Interface* **2022**, *14*, 24720–24728. (b) Olivieri, E.; Quintard, G.; Naubron, J.-V.; Quintard, A. Chemically Fueled Three-State Chiroptical Switching Supramolecular Gel with Temporal Control. *J. Am. Chem. Soc.* **2021**, *143*, 12650–12657. (c) Valentini, M.; Di Stefano, S.; Boekhoven, J. Coacervate-Droplet Cased Synthetic Cells Regulated by Activated Carboxylic Acids (ACAs). *ChemSystemsChem.* **2024**, *7*, No. e202400083.
- (8) (a) Del Giudice, D.; Spatola, E.; Valentini, M.; Ercolani, G.; Di Stefano, S. Dissipative Dynamic Libraries (DDLs) and Dissipative Dynamic Combinatorial Chemistry (DDCC). *ChemSystemsChem.* **2022**, *4*, No. e202200023. (b) Del Giudice, D.; Valentini, M.; Melchiorre, G.; Spatola, E.; Di Stefano, S. Dissipative Dynamic Covalent Chemistry (DDCvC) Based on the Transimination Reaction. *Chem. - Eur. J.* **2022**, *28*, No. e202200685.
- (9) (a) Berrocal, J. A.; Biagini, C.; Mandolini, L.; Di Stefano, S. Coupling of the Decarboxylation of 2-Cyano-2-phenylpropanoic Acid to Large-Amplitude Motions: A Convenient Fuel for an Acid–Base - Operated Molecular Switch. *Angew. Chem., Int. Ed.* **2016**, *55*, 6997–7001. (b) Erbas-Cakmak, S.; Fielden, S. D. P.; Karaca, U.; Leigh, D. A.; McTernan, C. T.; Tetlow, D. J.; Wilson, M. R. Rotary and linear molecular motors driven by pulses of a chemical fuel. *Science* **2017**, *358*, 340–343. (c) Biagini, C.; Albano, S.; Caruso, R.; Mandolini, L.; Berrocal, J. A.; Di Stefano, S. Variations in the fuel structure control the rate of the back and forth motions of a chemically fuelled molecular switch. *Chem. Sci.* **2018**, *9*, 181–188. (d) Biagini, C.; Capocasa, G.; Cataldi, V.; Del Giudice, D.; Mandolini, L.; Di Stefano, S. The Hydrolysis of the Anhydride of 2-Cyano-2-phenylpropanoic Acid Triggers the Repeated Back and Forth Motions of an Acid–Base Operated Molecular Switch. *Chem. - Eur. J.* **2019**, *25*, 15205–15211. (e) Ren, Y.; Jamagne, R.; Tetlow, D. J.; Leigh, D. A. A tape-reading molecular ratchet. *Nature* **2022**, *612*, 78–82. (f) Del Giudice, D.; Valentini, M.; Sappino, C.; Spatola, E.; Murru, A.; Ercolani, G.; Di Stefano, S. Controlling the Conformation of 2-Dimethylaminobiphenyls by Transient Intramolecular Hydrogen Bonding. *J. Org. Chem.* **2023**, *88*, 4379–4386.
- (10) Melchiorre, G.; Visieri, L.; Valentini, M.; Cacciapaglia, R.; Casnati, A.; Baldini, L.; Berrocal, J. A.; Di Stefano, S. Imine-Based Transient Supramolecular Polymers. *J. Am. Chem. Soc.* **2025**, *147*, 11327–11335.
- (11) Valentini, M.; Ercolani, G.; Di Stefano, S. How Activated Carboxylic Acids Can Drive Dissipative Systems. *ChemSystemsChem.* **2025**, *7*, No. e00021.

(12) Valentini, M.; Ercolani, G.; Di Stefano, S. Kinetic Trapping of an Out-of-Equilibrium Dynamic Library of Imines by Changing Solvent. *Chem. - Eur. J.* **2024**, *30*, No. e202401104.

(13) (a) Brunsfeld, L.; Folmer, B. J. B.; Meijer, E. W.; Sijbesma, R. P. Supramolecular Polymers. *Chem. Rev.* **2001**, *101*, 4071–4098. (b) Aida, T.; Meijer, E. W.; Stupp, S. I. Functional Supramolecular Polymers. *Science* **2012**, *335*, 813–817. (c) de Greef, T. F. A.; Meijer, E. W. Supramolecular polymers. *Nature* **2008**, *453*, 171–173.

(14) De Angelis, M.; Capocasa, G.; Ranieri, F.; Mazzocanti, G.; Fratello, F.; Manetto, S.; Fagnano, A.; Massera, C.; Olivo, G.; Ceccacci, F.; Ciogli, A.; Di Stefano, S. Transient Induction of Chirality from an Activated Carboxylic Acid to a Zinc Complex. *Angew. Chem., Int. Ed.* **2025**, *64*, No. e202513917.

(15) (a) Notti, A.; Pisagatti, I.; Nastasi, F.; Patané, S.; Parisi, M. F.; Gattuso, G. Stimuli-Responsive Internally Ion-Paired Supramolecular Polymer Based on a Bis-pillar[5]arene Dicarboxylic Acid Monomer. *J. Org. Chem.* **2021**, *86*, 1676–1684. (b) Aboudzadeh, M. A.; Muñoz, M. E.; Santamaria, A.; Fernández-Berridi, M. J.; Irusta, L.; Mecerreyes, D. Synthesis and Rheological Behavior of Supramolecular Ionic Networks Based on Citric Acid and Aliphatic Diamines. *Macromolecules* **2012**, *45*, 7599–7606.

(16) When  $H_2N(CH_2)_nNH_2$  ( $n = 5$  or  $6$ ) were used instead of diamine **3**, precipitation was observed immediately after mixing with diacid **1H<sub>2</sub>**, even at low concentrations. The introduction of oxygen atoms in the methylene chain connecting the two functional groups of **1H<sub>2</sub>**, which could have favored solubility, turned out to be challenging from a synthetic point of view.

(17) As a matter of fact, we previously showed that the crown ethers (thus, compounds containing oxygen atoms, see ref **10**) as well as competitive non protic solvents (acetonitrile, see ref **12**), strongly accelerate the decarboxylation of ACAs by weakening the carboxylate-ammonium ion-pairing.

(18) (a) Voorter, P. J.; McKay, A.; Dai, J.; Paravagna, O.; Cameron, N. R.; Junkers, T. Solvent-independent molecular weight determination of polymers based on a truly universal calibration. *Angew. Chem., Int. Ed.* **2022**, *61*, No. e202114536. (b) Ruzicka, E.; Pellechia, P.; Benicewicz, B. C. Polymer Molecular Weights via DOSY NMR. *Anal. Chem.* **2023**, *95*, 7849–7854.

(19) (a) Ciaccia, M.; Tosi, I.; Baldini, L.; Cacciapaglia, R.; Mandolini, L.; Di Stefano, S.; Hunter, C. A. Applications of dynamic combinatorial chemistry for the determination of effective molarity. *Chem. Sci.* **2015**, *6*, 144–151. (b) Timmerman, P.; Weidmann, J.-L.; Jolliffe, K. A.; Prins, L. J.; Reinhoudt, D. N.; Shinkai, S.; Frish, L.; Cohen, Y. NMR diffusion spectroscopy for the characterization of multicomponent hydrogen-bonded assemblies in solution. *J. Chem. Soc., Perkin Trans. 2* **2000**, 2077–2089. (c) Waldeck, A. R.; Kuchel, P. W.; Lennon, A. J.; Capman, B. E. NMR diffusion measurements to characterise membrane transport and solute binding. *Prog. Nucl. Magn. Reson. Spectrosc.* **1997**, *30*, 39–68.

(20) A cubic exponent gives unrealistically high values of DP that would require an intermolecular equilibrium constant  $K$  of the order of  $10^8 \text{ mol}^{-1} \text{ L}$  (vide infra). Such a value seems too high for a salt bridge in chloroform.

(21) The fact that the high concentrated solutions remain homogeneous on visual inspection for 2 days at 25 °C ensures that the precipitation phenomenon does not influence the initial DOSY measurements used to determine initial DP values.

(22) Jacobson, H.; Stockmayer, W. H. Intramolecular Reaction in Polycondensations. I. The Theory of Linear Systems. *J. Chem. Phys.* **1950**, *18*, 1600–1606.

(23) Ercolani, G.; Mandolini, L.; Mencarelli, P.; Roelens, S. Macrocyclization under thermodynamic control. A theoretical study and its application to the equilibrium cyclooligomerization of  $\beta$ -propiolactone. *J. Am. Chem. Soc.* **1993**, *115*, 3901–3908.

(24) (a) Kirby, A. J. Effective Molarities for Intramolecular Reactions. *Adv. Phys. Org. Chem.* **1980**, *17*, 183–278. (b) Illuminati, G.; Mandolini, L. Ring Closure Reactions of Bifunctional Chain Molecules. *Acc. Chem. Res.* **1981**, *14*, 95–102. (c) Mandolini, L. Intramolecular Reactions of Chain Molecules. *Adv. Phys. Org. Chem.*

**1986**, *22*, 1–111. (d) Di Stefano, S.; Ercolani, G. Equilibrium Effective Molarity As a Key Concept in Ring-Chain Equilibria, Dynamic Combinatorial Chemistry, Cooperativity and Self-assembly. *Adv. Phys. Org. Chem.* **2016**, *50*, 1–76. (e) Motloch, P.; Hunter, C. A. Thermodynamic Effective Molarities for Supramolecular Complexes. *Adv. Phys. Org. Chem.* **2016**, *50*, 77–118. (f) Di Stefano, S.; Mandolini, L. The canonical behavior of the entropic component of thermodynamic effective molarity. An attempt at unifying covalent and noncovalent cyclizations. *Phys. Chem. Chem. Phys.* **2019**, *21*, 955–987.

(25) Truesdell, C. On a Function Which Occurs in the Theory of the Structure of Polymers. *Ann. Math.* **1945**, *46*, 144–157.

(26) (a) Kumar, S.; Nussinov, R. Salt bridge stability in monomeric proteins. *J. Mol. Biol.* **1999**, *293*, 1241–1255. (b) Ban, X.; Lahiri, P.; Dhoble, A. S.; Li, D.; Gu, Z.; Li, C.; Cheng, L.; Hong, Y.; Li, Z.; Kaustubh, B. Evolutionary Stability of Salt Bridges Hints Its Contribution to Stability of Proteins. *Comput. Struct. Biotechnol. J.* **2019**, *17*, 895–903.



CAS INSIGHTS™

EXPLORE THE INNOVATIONS  
SHAPING TOMORROW

Discover the latest scientific research and trends with CAS Insights. Subscribe for email updates on new articles, reports, and webinars at the intersection of science and innovation.

Subscribe today

CAS  
A division of the  
American Chemical Society